ORIGINAL RESEARCH

Combined Diffusion Imaging and MR Spectroscopy in the Diagnosis of Human Prion Diseases

D. Galanaud
S. Haik
M.G. Linguraru
J.-P. Ranjeva
B. Faucheux
E. Kaphan
N. Ayache
J. Chiras
P. Cozzone
D. Dormont
J.-P. Brandel

BACKGROUND AND PURPOSE: The physiopathologic bases underlying the signal intensity changes and reduced diffusibility observed in prion diseases (TSEs) are still poorly understood. We evaluated the interest of MRS combined with DWI both as a diagnostic tool and a way to understand the mechanism underlying signal intensity and ADC changes in this setting.

MATERIALS AND METHODS: We designed a prospective study of multimodal MR imaging in patients with suspected TSEs. Forty-five patients with a suspicion of TSE and 11 age-matched healthy volunteers were included. The MR imaging protocol included T1, FLAIR, and DWI sequences. MRS was performed on the cerebellum, pulvinar, right lenticular nucleus, and frontal cortex. MR images were assessed visually, and ADC values were calculated.

RESULTS: Among the 45 suspected cases, 31 fulfilled the criteria for probable or definite TSEs (19 sCJDs, 3 iCJDs, 2 vCJDs, and 7 genetic TSEs); and 14 were classified as AltDs. High signals in the cortex and/or basal ganglia were observed in 26/31 patients with TSEs on FLAIR and 29/31 patients on DWI. In the basal ganglia, high DWI signals corresponded to a decreased ADC. Metabolic alterations, increased mIns, and decreased NAA were observed in all patients with TSEs. ADC values and metabolic changes were not correlated; this finding suggests that neuronal stress (vacuolization), neuronal loss, and astrogliosis do not alone explain the decrease of ADC.

CONCLUSIONS: MRS combined with other MR imaging is of interest in the diagnosis of TSE and provides useful information for understanding physiopathologic processes underlying prion diseases.

ABBREVIATIONS: ADC = apparent diffusion coefficient; AltD = alternative diagnosis; Avg = average; C (or c) = control; Cho = choline; CJD = Creutzfeldt-Jakob disease; Cr = creatine; DWI = diffusion-weighted imaging; EEG = electroencephalograph; FFI = fatal familial insomnia; FLAIR = fluid-attenuated inversion recovery; GABA = gamma-aminobutyric acid; gCJD = genetic CJD; Glx = glutamine-glutamate-GABA; GSS = Gerstmann Strausser Sheinker syndrome; iCJD = iatrogenic CJD; mIns = myo-inositol; MM = methionine homozygosity (*PRNP*: genotype at codon 129); MRS = MR spectroscopy; MRI = MR imaging; MV = methionine-valine heterozygosity (*PRNP*: genotype at codon 129); NA = data not available; NAA = *N*-acetylaspartate; NS = not significant or nonspecific slow waves; P (or p) = patient; *PRNP* = genotype at codon 129; *PrP* = prion protein or persistent plexus gene; S = sum of metabolites; sCJD = sporadic CJD; TSE = human transmissible spongiform encephalopathy; vCJD = variant CJD; VV = valine homozygosity (*PRNP*: genotype at codon 129)

MR imaging has become a tool of choice in the diagnosis of several forms of prion diseases (TSEs). The presence of areas of increased signal intensity, usually associated with a decreased ADC, are frequently observed on the cortex, thalamus, and/or basal ganglia of patients with sCJD, vCJD, or iCJD. However, the exact physiopathologic processes underlying these changes are still subject to debate. They have been variously attributed to the *PrP* deposits, the morphologic changes of neurons, or gliosis.[1-3] Correlation of these signal-intensity changes with pathologic data is further impaired by their modification during the time course of the disease.[4-6] MRS can, on the other hand, be performed simultaneously with conventional imaging and can give information on the ongoing pathologic processes: Neuronal loss or stress will lead to a decrease in NAA, while gliosis will induce an increase in the resonance of mIns. Hence, to determine the diagnostic value of MRS in TSEs and to better understand the physiopathologic processes underlying the signal intensity/ADC changes, we prospectively studied 45 patients clinically suspected of having prion diseases with a multimodal MR imaging protocol, including MRS and conventional and diffusion imaging.

Materials and Methods

This prospective study was approved by the committee on ethics of La Timone Hospital. Patients (or their representatives) and controls gave written informed consent to participate in the study.

Received August 19, 2009; accepted after revision December 13.

From the Departments of Neuroradiology (D.G., J.C., D.D.) and Pathology (S.H., B.F.), Cellule de référence des maladies à prions (S.H., J.-P.B.) Pitié-Salpêtrière Hospital, Paris, France; INSERM UMRS 975 CNRS UMR 7225 centre de recherche de l'institut du cerveau et de la moëlle épinière (D.D., D.G., S.H., B.F., J.-P.B.), Pitié Salpêtrière Hospital, Paris, France; Université Pierre et Marie Curie, Paris 6 (D.G., D.D., J.C., L.P.), France; CRMBM-CEMEREM, UMR CNRS 6612 (J-P.R., P.C.), Faculté de Médecine La Timone and Department of Neurology (E.K.), La Timone Hospital Marseille, France; Epidaure/Asclepios Research Group (M.G.L., N.A.), Institut National de Recherche en Informatique et Automatique, Sophia Antipolis, France; and Department of Radiology and Imaging Sciences (M.G.L.), Clinical Center, National Institutes of Health, Bethesda, Maryland.

This work was supported by a grant from the Groupement d'intérêt spécifique "Prions." Other financial support for this work was provided by the French Ministry of Research, the Centre National de la Recherche Scientifique, and the Institut Universitaire de France.

Please address correspondence to Damien Galanaud, MD, Department of Neuroradiology, Pitié Salpêtrière Hospital, 47 Blvd de l'Hôpital, F-75013 Paris, France; e-mail: galanaud@ dat.org

DOI 10.3174/ajnr.A2069

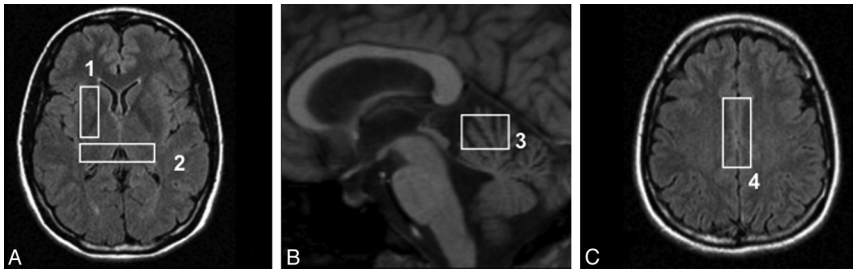

Fig 1. Location of the MRS voxels on axial FLAIR (*A* and *C*) and sagittal T1-weighted (*B*) sequences: lenticular nucleus (1), pulvinar (2), cerebellar vermis (3), and frontal cortex (4).

Selection and Classification of Patients

Patients were referred to the neurology departments of La Pitié Salpêtrière (Paris) and La Timone hospital (Marseille) for suspicion of TSEs (sporadic, genetic, iatrogenic, or variant). This diagnosis was reassessed by 2 neurologists who were experts in prion diseases (J.-P.B. and S.H.). Patients then underwent a multimodal MR imaging, which was part of an extensive evaluation, including 14.3.3 protein detection in the CSF, EEG, and genotyping of the *PrP* gene. Tonsil biopsies were performed when vCJD was suspected. Postmortem examination was performed in 9 subjects. The eventual diagnosis was based on the World Health Organization clinical diagnostic criteria for prion diseases.[7] The pathologic findings in the patient with FFI were published in a previous article.[8]

MR Imaging Protocol

MR imaging examinations were performed on 1.5T magnets at La Pitié Salpêtrière, Paris (Signa HDx; GE Healthcare, Milwaukee, Wisconsin) and at La Timone Hospital, Marseille (Vision; Siemens, Erlangen, Germany). Patients were given a light sedation with hydroxyzine dichlorhydrate, 100 mg, when required by their clinical status. Pulse saturometry was monitored during the procedure. Total time inside the magnet was approximately 1 hour. The MR imaging protocol included the following:

1) A sagittal T1-weighted sequence.
2) One axial T1-weighted sequence (TR = 644 ms, TE = 15 ms, 3-mm thickness, interleaved).
3) An axial FLAIR sequence (TR = 8000 ms, TI = 2200 ms, TE = 110 ms, 5-mm thickness, interleaved).
4) DWI (single-shot echo-planar imaging sequence; $b = 0, 500, 1000$ s/mm^2 applied in the *x, y,* and *z* directions sequentially; 19 sections; 5-mm thickness; matrix = 128 × 128; FOV = 256 × 256 mm^2). ADC maps were reconstructed by using this sequence as previously described.[9]
5) Four stimulated echo acquisition mode single-voxel spectroscopy acquisitions (TR = 1500 ms, TE = 20 ms, TM = 30 ms) on regions known to be frequently involved in prion diseases: the cerebellar vermis (voxel size, 20 × 20 × 15 mm), the pulvinar (voxel location as previously described[10]), the right lenticular nucleus (voxel size, 35 × 15 × 15 mm), and the bifrontal cortex (voxel size, 40 × 20 × 15 mm). The locations of the voxels are shown on Fig 1.

Processing of MR Images and Spectra

MR images were analyzed with 2 methods:

1) MR imaging examinations were interpreted by 2 expert neuroradiologists (D.G. and D.D.). Signal intensity on FLAIR and DWIs was evaluated side by side in cortical regions (frontal, temporoinsular, and parieto-occipital) and 3 areas of the basal ganglia (caudate, putamen, and thalamus). Signal intensity was ranked from 1 to 4 as follows: 1, normal; 2, dubious area of increased signal intensity; 3, obvious area of increased signal intensity; and 4, area of markedly increased signal intensity. Differences between observers were settled by consensus.
2) ADC values were calculated by using the software provided by the manufacturers in the following locations: head of the caudate nuclei, putamen, thalamus, and pulvinar. ADC regions were drawn on the DWI image, on the section on which each nucleus had the greatest extension. The voxel included the whole structure present on this section minus the pixels closest to the ventricles, to avoid partial volume effect. Because of partial volume effects, we did not calculate the ADC in the cerebellum and frontal cortex.

Quantification of MR Spectra

The MRS data were analyzed by using a dedicated software described elsewhere.[11] Resonances were assigned according to those described in the literature.[12,13] Spectra were processed as previously described.[14,15] Briefly, we manually corrected the baselines and integrated the resonances of the following metabolites: NAA, Cr, Cho, mIns, and Glx. The value of each metabolite was then divided by the sum (S = NAA + Cr + Cho + mIns + Glx) of all metabolite values (semiquantitative evaluation). This semiquantitative analysis, the sum of metabolites, was preferred to the calculation of individual metabolite ratios (eg, NAA/Cr or Cho/Cr), which are dependent on both numerator and denominator variations. For instance, a decreased NAA/Cr ratio could be attributed to both a reduction in NAA (resulting from neuronal stress) or an increase in Cr (resulting from a glial activation or proliferation).[16-18] Ratios of the sum of metabolites "smoothen" these variations and enable a better evaluation of the variations of the metabolite in the numerator. However, we did evaluate the mIns/NAA ratio. Because NAA is a neuronal marker and mIns is a glial marker, this ratio simultaneously evaluates neuronal stress/death and gliosis, which are 2 of the main histologic landmarks of prion diseases. The presence of detectable free lipids and lactate was also assessed.

Statistical Analysis

Statistical analysis was performed by using the JMP software (SAS Institute, Cary, North Carolina). Differences among patients, volunteers, and AltDs were determined by a Kruskal-Wallis analysis followed by a Scheffé test with a Bonferroni correction for multiple comparisons. The statistical analysis was also performed on the subgroup of patients with sCJD, who were compared with controls by using an unpaired Student *t* test. Due to the small numbers and heterogeneity of the other subtypes of CJD and AltDs, no further statistical analysis could be performed on these patients and their metabolic anomalies were only described.

Table 1: Main clinical and paraclinical data of patients

No.	Form	Age (yr)	*PRNP*	EEG[a]	14.3.3[b]	Duration[c]	MRI Delayed[d]
1	FFI[e]	54	MM D178N-129 mol/L	NS	–	6	5
2	gCJD[e]	69	MM E200K	+	+	4	6
3	gCJD[e]	58	MM E200K	+	NA	6	3
4	gCJD[e]	49	MV D178N-129V	–	–	10+	4
5	gCJD[e]	70	MV V203I	NS	+	11	10
6	gCJD[e]	67	MM E200K	NA	NA	5	3
7	iCJD	18	MV	NA	–	16	6
8	iCJD	34	MV	+	+	23	8
9	iCJD[e]	25	MM	–	–	12	8
10	GSS[e]	47	MV P102 L	–	–	54	27
11	vCJD	43	MM	+	–	15	12
12	vCJD	52	MM	NS	–	8	7
13	sCJD	66	NA	NA	NA	NA	3
14	sCJD[e]	54	MV	+	+	10	6
15	sCJD[e]	62	MM	+	+	19	7
16	sCJD[e]	66	VV	+	+	4	2
17	sCJD[e]	51	MM	+	+	4	2
18	sCJD	56	MV	–	+	13	8
19	sCJD	74	MM	NA	NA	3	2
20	sCJD	52	MM	+	+	3	2
21	sCJD[e]	81	MM	+	+	4	4
22	sCJD	53	MV	NS	+	21	1
23	sCJD	55	MV	+	–	60+	23
24	sCJD	80	MV	+	–	9	8
25	sCJD	77	MV	+	–	24+	10
26	sCJD	40	NA	NA	NA	10+	9
27	sCJD	72	MM	+	+	3	2
28	sCJD[e]	64	MM	+	+	4	1
29	sCJD	55	NA	–	+	26	20
30	sCJD	84	NA	NA	NA	5	3
31	sCJD	80	NA	NS	–	2	1

Note:— – indicates not present.
[a] + Indicates periodic sharp wave complexes.
[b] Detection of 14.3.3 protein in the CSF.
[c] Duration of the disease in months.
[d] Time in months between first symptoms and MR imaging examination.
[e] The diagnosis was confirmed by postmortem examination and/or mutation was present in the *PRNP*. *PRNP*: genotype at codon 129 (MM, VV, MV) and mutation when present.

Results

Forty-five patients were prospectively studied. The diagnosis of prion diseases was eventually confirmed in 31 subjects and included 1 FFI, 1 GSS, 2 vCJD, 3 iCJD related to growth hormone treatment of CJD, 5 gCJD, and 19 sCJD. The mean time between first symptoms and the MR imaging examination was 7 months. The median duration of disease in sCJD was 7 months. Genotype at codon 129 of the *PRNP* gene was determined in 29/31 subjects. The patients' main clinical and paraclinical characteristics are shown in Table 1.

The diagnoses for the other 14 patients were the following: 2 Alzheimer diseases, 1 vascular dementia, 1 Hashimoto encephalitis, 1 depression, 1 metabolic, 1 epileptic encephalopathy, 1 atypical Parkinson disease, 1 paraneoplastic syndrome, and 5 dementias of unknown etiology.

Conventional Imaging

High signals in the cortex and/or basal ganglia were observed in 26/31 patients with TSEs on FLAIR sequence. The 5 patients with normal findings on the FLAIR sequence were the ones with FFI and the GSS, 1/19 sCJD and 1/3 iCJD, and 1 codon 200 mutation of the 5 cases of gCJD.

On the DWI sequence, 29/31 patients had abnormalities: 26/31 on the cortical areas and 25/31 on the basal ganglia. The 3 patients with normal FLAIR findings and lesions on the DWI

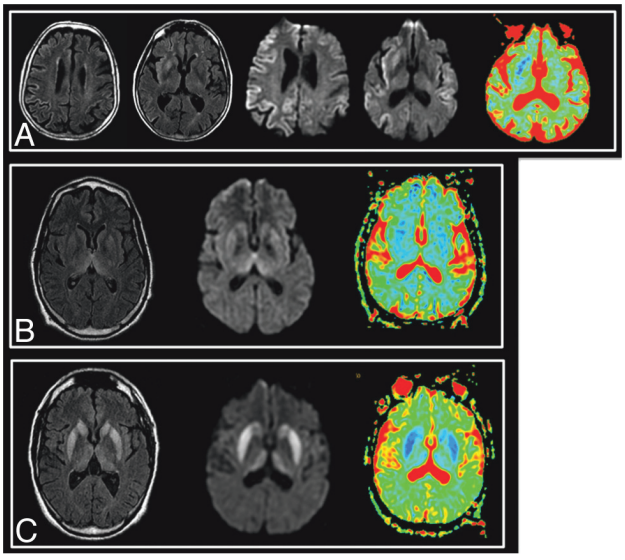

Fig 2. Typical images in cases of sCJD (*A*), vCJD (*B*), and gCJD (*C*). FLAIR, DWI, and ADC map, respectively, are shown. Areas of increased signal intensity, which involve the cortex and the striatum are more extensive and more clearly visible on diffusion images. On the basal ganglia, these changes are associated with a decreased ADC. There is widespread involvement of the cortex in the patient with sCJD. gCJD and vCJD both present with lesions of the thalamus and lenticular nuclei. However, in the variant case, as opposed to the genetic one, the areas of high signal intensity are more pronounced in the pulvinar than in the striatum as has been previously described in this phenotype.

Table 2: Number of patients presenting with areas of significant (≥3 on the visual scale) increased signal/decreased ADC in the different brain structures[a]

$N = 31$	FLAIR	DWI
Frontal	17	25
Parietal	15	18
Temporal	14	18
Occipital	11	13
Insula	11	15
Cortex, all	19	26
Lenticular	18	23
Caudate	16	23
Thalamus	6	11
Basal ganglia, all	20	25
Brain stem	1	2
Global	26	29

[a] The most frequently involved cerebral lobes are the frontal, the temporal, and the parietal. In the deep brain structures, the lenticular and the caudate nuclei are affected in a similar number of patients

sequence were the patient with gCJD, who presented clear abnormalities on both cortical areas and basal ganglia; the one with sCJD, who had widespread involvement of the cortex; and the one with iatrogenic CJD, who had clear involvement of the striatum.

Neither patients with an AltD nor the control subjects had areas of increased signal intensity or reduced diffusibility in the cortex or basal ganglia.

Typical images are shown on Fig 2. The frequency of involvement of the major brain structures is summarized on Table 2.

ADC Values

ADC values were significantly reduced in the head of the caudate nuclei, thalamus, pulvinar, and lenticular nuclei in patients with prion disease compared with controls ($P < 10^{-2}$ in all cases). This difference was also present when the analysis was restricted to subjects with sCJD.

In patients with AltDs, ADC values were not significantly different from those of controls.

MRS

A summary of MRS results is given in On-line Table 1. Typical spectra are shown in Fig 3. MRS could be performed in all patients and controls. Some spectra had to be excluded because of poor quality in 1 control (lenticular voxel) and 2 patients with CJD (a pulvinar acquisition in a patient with sCJD and a lenticular acquisition in the patient with FFI). No difference was observed in the metabolic ratios between the controls in the 2 MR imaging centers.

The NAA/S, the mIns/S, and mIns/NAA ratios showed differences in the global (Kruskal-Wallis) analysis. No other metabolic ratio was significantly different between groups. The NAA/S ratio was lower and the mIns/S and mIns/NAA ratios were higher in patients with prion disease compared with controls in most studied voxels (On-line Table 1). The mIns/NAA ratio was the only one to be significantly different in all 4 voxels (Fig 4).

In the lenticular and pulvinar nuclei, where both MRS was performed and ADC values could be calculated, no metabolic ratio was significantly correlated to ADC values (Fig 5), regardless of the presence of areas of increased signal intensity in FLAIR or DWI.

No parameter on DWI or MRS was correlated to the survival of the patients.

Discussion

While the value of MR imaging for the diagnosis of most subtypes of prion diseases has been well established in several large retrospective studies, the pathologic bases of the observed signal-intensity changes on diffusion and T2/FLAIR images are still imperfectly understood. Correlating signal intensity or ADC changes with the findings at autopsy is of crucial importance but should be complemented by in vivo studies because it is known that the pattern of lesions on MR imaging can change during the course of the disease,[4,6,19,20] and because the interval between MR imaging and death is often long. MRS is a noninvasive method to study brain metabolism, which can be performed during the same examination as diffusion imaging and can thus allow the synchronous evaluation of diffusion lesions and cellular changes.

The MRS results in our study are in accordance with the classic pathologic findings in prion diseases. The metabolic alterations are a decrease in NAA/S, which corresponds to neuronal stress and death, and an increase in mIns/S, which is a marker of gliosis. To our knowledge, this study is the first prospective evaluation of MRS in human prion diseases. Our findings are similar to those reported in previously published articles of human and animal models of prion diseases.[4,10,21-27] We did not observe any correlation between ADC values and any metabolic ratio. This does not support neuronal stress such as vacuolization (spongiform changes) as the main factor that could explain a reduced diffusibility of water.[28] Because gliosis increases ADC,[3] we can speculate a role for *PrP* deposits in the decrease of ADC. The normalization of the ADC values observed in some patients later in the course of the disease could be explained at least in part by the subsequent development of gliosis.[8] This hypothesis could be verified with follow-up examinations, which could show an increase in mIns. However, while they were initially intended in our study, they could not be performed due to the rapidly worsening clinical condition of most patients. A specific postmortem study of radiopathologic correlations with extensive quantification of tissue alterations, including spongiform change, astrogliosis, microglial activation, and neuronal loss together with an assessment of abnormal protein accumulation, will help to better understand the pathologic supports of each neuroradiologic perturbation. The distinct prion-related lesions may influence differently, and sometimes with opposite effects, each MR imaging component.

The high frequency of metabolic alterations on MRS in patients with prion diseases can be explained by the targeting of MRS to the regions most commonly affected by these diseases. However, metabolic alterations were not present in all 4 locations in every patient. This is in accordance with the heterogeneous distribution of the pathologic changes in these diseases.[29] In addition, variations in NAA and mIns were also not systematically associated and could be found separately. These results are in agreement with the pathologic pattern of prion diseases, which diversely associates neuronal impairment and gliosis and varies among brain regions.

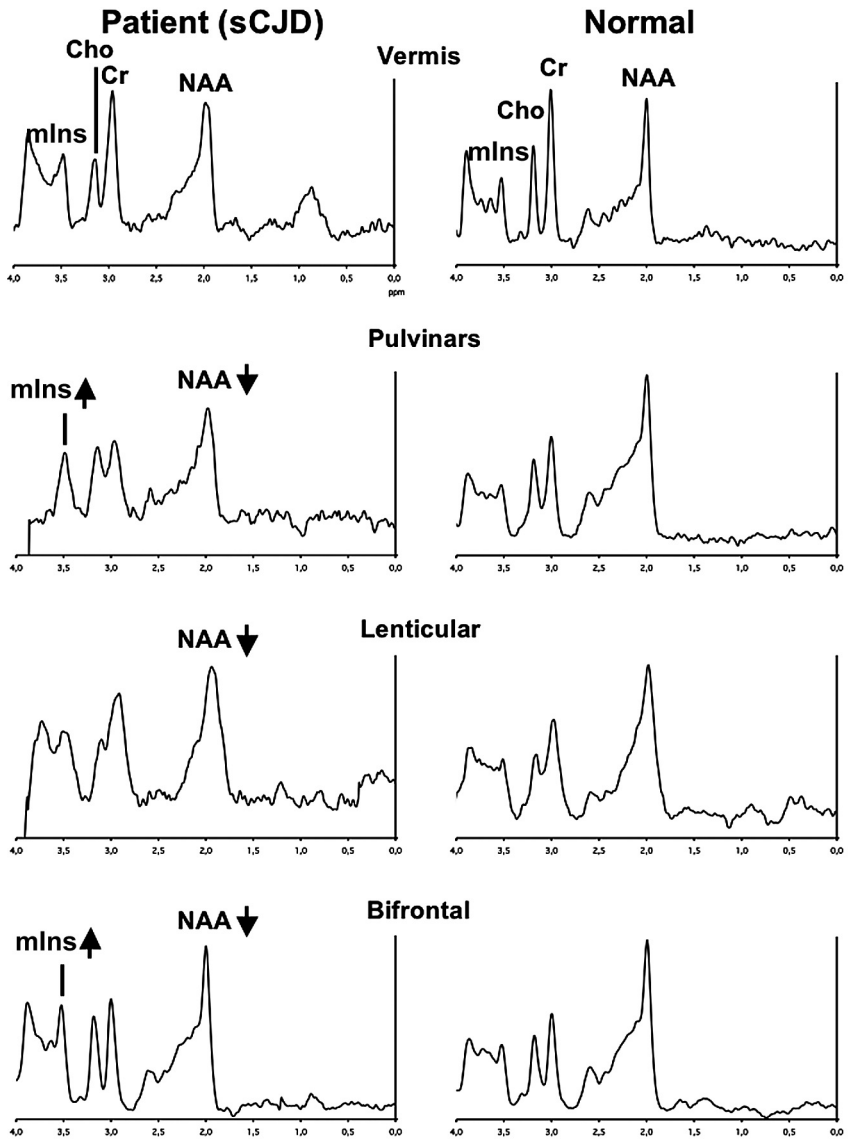

Fig 3. Typical spectra recorded in a patient with sCJD (left column) and in a healthy volunteer (right column) in the vermis, pulvinar, right lenticular nucleus, and frontal gray matter. Metabolic anomalies are observed on the bifrontal voxel (decreased NAA and increased mIns), on the lenticular voxel (decreased NAA), and on the bipulvinar voxel (decreased NAA and increased mIns). Note that to get an accurate idea of NAA and mIns variations, one should compare their resonances with "stable" metabolites (eg, Cr).

The coherence of these results with the pathologic data is reinforced by the findings in some subtypes: In the 2 cases of vCJD, the most severely affected areas were the pulvinars,[30] with a marked decrease in NAA/S and increase in mIns/S ratios, with vCJD being characterized by the occurrence of severe neuronal loss with intense gliosis in this region. In addition, the 3 patients with iCJD exhibited stronger decreased NAA/S in the cerebellum compared with the population with sCJD. This is in agreement with the early and predominant cerebellar symptoms and the neuropathologic patterns that are regularly observed in this form.[31]

We observed a higher sensitivity of FLAIR (84%) than was previously reported by Tschampa et al[32] in a large retrospective study (47%) of patients from different institutions. This can probably be explained by a homogeneous acquisition protocol on similar MR imaging magnets in our study.

The sensitivity (94%) of diffusion imaging was higher than previously observed in retrospective studies[32,33] and similar (92.3%) to the only prospective study that evaluated DWI in prion diseases so far.[34] This sequence is thus clearly the most sensitive among conventional MR imaging acquisitions for the diagnosis of prion diseases. The 2 cases with negative findings were genetic forms (1 FFI and 1 GSS). All cases of sCJD, gCJD, and iCJD had abnormalities on the DWI sequence. No patient with an AltD had areas of decreased ADC, confirming the high specificity of DWI for the diagnosis of prion diseases in the clinical setting of dementia of rapid onset.

One of 19 patients with sCJD had no lesions on the FLAIR sequence. The cortex was involved in 16/19 patients and the basal ganglia, in 13/19. All patients had areas of increased signal intensity on DWI, involving the cortex (19/19) and the basal ganglia (15/19). The distribution of lesions among the cortex and basal ganglia was similar to the one reported recently by Meissner et al.[35] Results of the analysis of MRS and

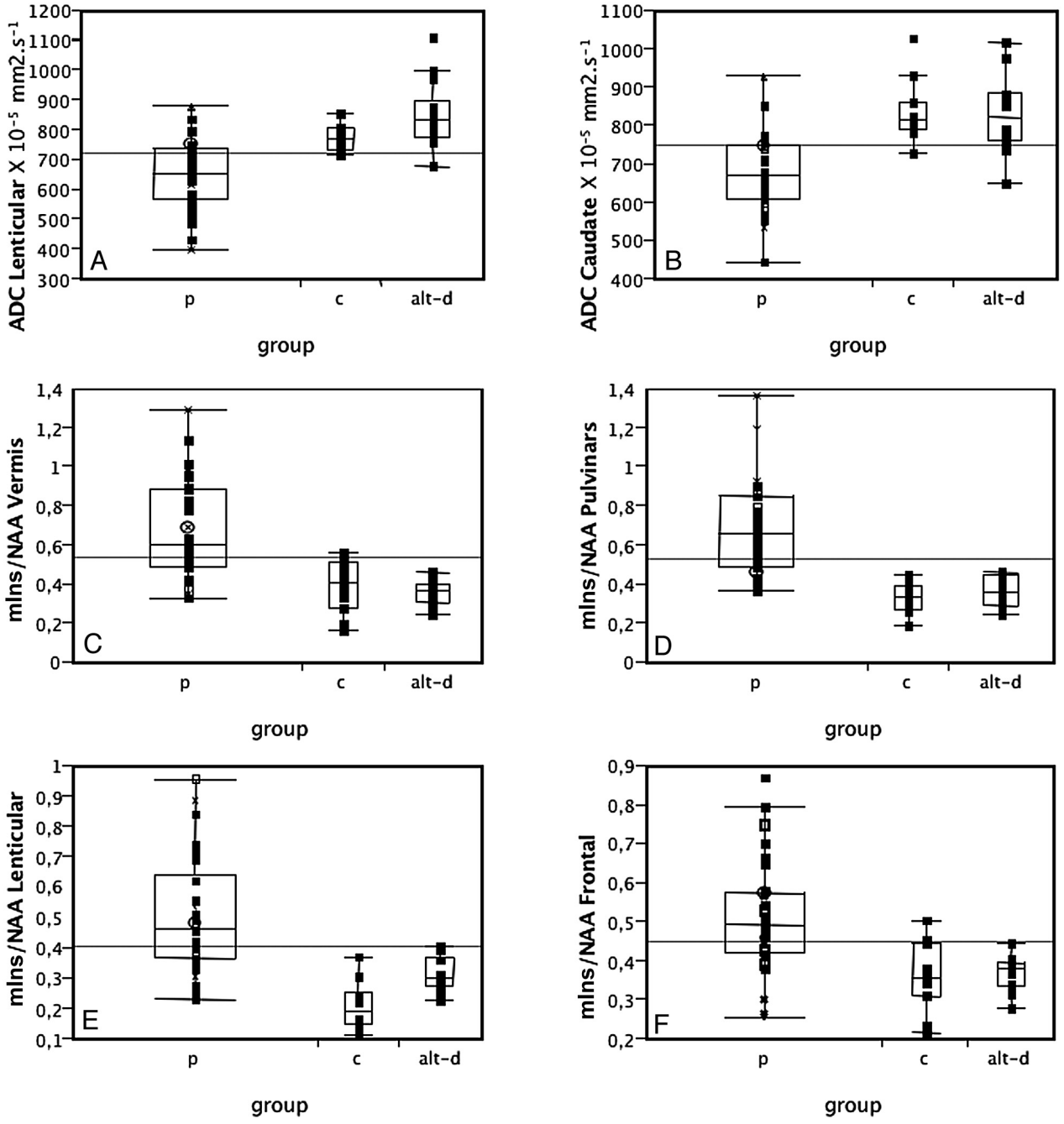

Fig 4. ADC values in the lenticular (*A*) and caudate (*B*) nuclei and mIns/NAA ratios on the vermis (*C*), pulvinar (*D*), right lenticular nucleus (*E*), and frontal gray matter (*F*) in patients with prion disease (p), controls (c), and those with AltD. ADC is decreased and mIns/NAA is increased in patients with prion disease compared with both controls and AltDs. Neither ADC values nor the mIns/NAA ratios can discriminate between the 2 latter groups.

ADC data performed on this subgroup of patients were comparable to those of the total group of patients with prion diseases (On-line Table 1).

Among the 17 patients with sCJD for which the genotype of *PRNP* at codon 129 was available, 9 had the MM; 7, the MV; and 1, the VV phenotype. Median duration of the disease was 4 months for the MM phenotype and 11.5 months for patients with MV and VV phenotypes. On FLAIR imaging, lesions of the basal ganglia were more frequent in patients with the MV or VV (7/8) phenotypes than in subjects with the MM (4/9) phenotype.

MR imaging findings in gCJD were heterogeneous. The patient with mutation D178N-129V had extensive areas of increased signal intensity on the cortex, on both FLAIR and DWI, with only minimal involvement of the basal ganglia (hypersignal of the left caudate). One patient with mutation 200 had no abnormalities on the FLAIR sequence but showed areas of hypersignal on the DWI sequences in the left striatum and frontal and insular cortices. The 2 other patients with mutation 200 had marked hypersignals in the striatum on both FLAIR and DWI imaging. Involvement of the cortex was also present on DWI. These results (frequency of involvement

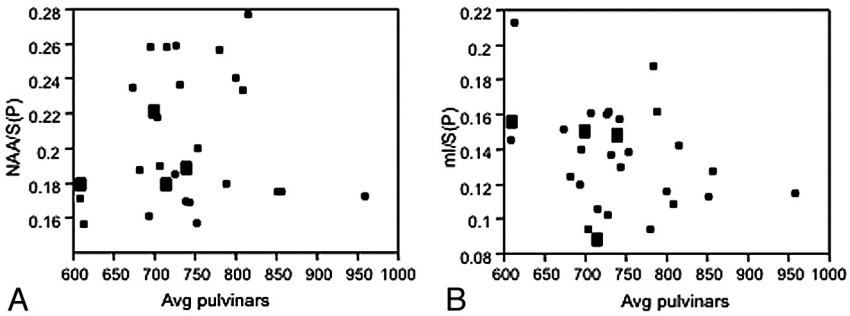

Fig 5. ADC values plotted against the NAA/S (*A*) and mIns/S (*B*) ratios measured on the same area of the pulvinar in patients with prion disease. There is an absence of correlation between these parameters ($R^2 = 0.003$, $P = .8$ and $R^2 = 0.11$, $P = .08$ respectively).

of the basal ganglia and cortical lesions detected on DWI) are comparable with those previously described in a population of subjects with mutation 200.[36] The patient with mutation V203I had diffuse lesions on both the cortex and basal ganglia. ADC values were diminished in the basal ganglia of all patients. Spectroscopic findings in the 5 genetic cases were similar to those of sporadic cases.

Among patients with iCJD, FLAIR imaging findings were normal in 1 patient; showed lesions restricted to the striatum in 1; and evidenced widespread involvement of the striatum, thalamus, periaqueductal gray matter, and cortex in another. On DWI, all patients showed marked areas of increased signal intensity in the striatum, which were associated with decreased ADC values. The 3 cases of iCJD had in common a markedly reduced NAA/S in the cerebellar vermis. MRS results were otherwise heterogeneous.

We observed the classic imaging pattern of vCJD, with hypersignals of the basal ganglia in both FLAIR and DWI sequences, predominating in the pulvinar (pulvinar sign). No lesions were seen on the cortex. The 2 patients with vCJD had similar spectroscopic findings, in accordance with previously published reports of MRS in this disease by the authors (about a previous patient) and others.[10,21,26] A pronounced decrease in NAA/S and an increase in mIns/S were present in the pulvinar. The metabolic abnormalities in the lenticular nuclei were limited to an increase in mIns, and the metabolic profiles of the vermis and the frontal cortex were both normal.

The patient with FFI had normal findings on FLAIR and DWI. Most interesting, as opposed to all other cases of prion diseases, ADC values were increased in the thalamus compared with those in healthy volunteers. MRS showed a decrease in NAA/S on the pulvinar, associated with an increased mIns/S. The metabolic profiles of the frontal cortex and of the vermis were normal, and the lenticular nucleus was not interpretable.

The patient with GSS had normal findings on FLAIR and DWI, except a moderate cerebellar atrophy. ADC values were within the normal range in all the locations studied. MRS showed diffuse changes overall similar to those of patients with sCJD. The most striking abnormality was a pronounced decrease in NAA/S in the lenticular nucleus.

Conclusions

Metabolic changes were detected in all patients with sporadic, inherited, or infectious prion diseases in at least 1 of the studied voxels, even in areas that looked normal on conventional imaging. In addition, we confirm, in this prospective study, that DWI has the highest sensitivity (94%) among the conventional MR imaging sequences. No metabolic ratio was correlated to ADC values, indicating that these 2 imaging modalities explore different pathologic processes. It should now be of great interest to confirm the specificity of DWI and MRS by a study on a large non-CJD population with dementia and to explore further the neuropathologic bases of MR imaging alterations in humans and in experimental in vivo models of prion diseases.

Acknowledgments

The authors are indebted to the patients who took part in this study and their families.

References

1. Bahn MM, Parchi P. **Abnormal diffusion-weighted magnetic resonance images in Creutzfeldt-Jakob disease.** *Arch Neurol* 1999;56:577–83
2. Finkenstaedt M, Szudra A, Zerr I, et al. **MR imaging of Creutzfeldt-Jakob disease.** *Radiology* 1996;199:793–98
3. Haik S, Dormont D, Faucheux BA, et al. **Prion protein deposits match magnetic resonance imaging signal abnormalities in Creutzfeldt-Jakob disease.** *Ann Neurol* 2002;51:797–99
4. Oppenheim C, Zuber M, Galanaud D, et al. **Spectroscopy and serial diffusion MR findings in hGH-Creutzfeldt-Jakob disease.** *J Neurol Neurosurg Psychiatry* 2004;75:1066–69
5. Tribl GG, Strasser G, Zeitlhofer J, et al. **Sequential MRI in a case of Creutzfeldt-Jakob disease.** *Neuroradiology* 2002;44:223–26
6. Ukisu R, Kushihashi T, Kitanosono T, et al. **Serial diffusion-weighted MRI of Creutzfeldt-Jakob disease.** *AJR Am J Roentgenol* 2005;184:560–66
7. Brandel JP, Delasnerie-Laupretre N, Laplanche JL, et al, **Diagnosis of Creutzfeldt-Jakob disease: effect of clinical criteria on incidence estimates.** *Neurology* 2000;54:1095–99
8. Haik S, Galanaud D, Linguraru MG, et al. **In vivo detection of thalamic gliosis: a pathoradiologic demonstration in familial fatal insomnia.** *Arch Neurol* 2008;65:545–49
9. Nicoli F, Lefur Y, Denis B, et al. **Metabolic counterpart of decreased apparent diffusion coefficient during hyperacute ischemic stroke: a brain proton magnetic resonance spectroscopic imaging study.** *Stroke* 2003;34:e82–87
10. Galanaud D, Dormont D, Grabli D, et al. **MR spectroscopic pulvinar sign in a case of variant Creutzfeldt-Jakob disease.** *J Neuroradiol* 2002;29:285–87
11. Galanaud D, Le Fur Y, Nicoli F, et al. **Regional metabolite levels of the normal posterior fossa studied by proton chemical shift imaging.** *MAGMA* 2001;13:127–33
12. Frahm J, Bruhn H, Gyngell M, et al. **Localized proton spectroscopy using stimulated echoes: initial application to human brain in vivo.** *Magn Reson Med* 1989;9:79–93
13. Michaelis T, Merboldt K, Hänicke W, et al. **On the identification of cerebral metabolites in localized H-1 NMR spectra of the human brain in vivo.** *NMR Biomed* 1991;4:90–98
14. Confort-Gouny S, Vion-Dury J, Nicoli F, et al. **A multiparametric data analysis showing the potential of localized proton MR spectroscopy in the brain in the metabolic characterization of neurological diseases.** *J Neurol Sci* 1993; 118:123–33
15. Galanaud D, Nicoli F, Chinot O, et al. **Noninvasive diagnostic assessment of**

brain tumors using combined in vivo MR imaging and spectroscopy. *Magn Reson Med* 2006;55:1236–45
16. Chang L, Ernst T, Osborn D, et al. **Proton spectroscopy in myotonic dystrophy.** *Arch Neurol* 1998;55:305–11
17. Fernando KT, McLean MA, Chard DT, et al. **Elevated white matter myo-inositol in clinically isolated syndromes suggestive of multiple sclerosis.** *Brain* 2004;127:1361–69
18. Vrenken H, Barkhof F, Uitdehaag BM, et al. **MR spectroscopic evidence for glial increase but not for neuro-axonal damage in MS normal-appearing white matter.** *Magn Reson Med* 2005;53:256–66
19. Matoba M, Tonami H, Miyaji H, et al. **Creutzfeldt-Jakob disease: serial changes on diffusion-weighted MRI.** *J Comput Assist Tomogr* 2001;25:274–77
20. Krasnianski A, Kallenberg K, Collie DA, et al. **MRI in the classical MM1 and the atypical MV2 subtypes of sporadic CJD: an inter-observer agreement study.** *Eur J Neurol* 2008;15:762–71
21. Pandya HG, Coley SC, Wilkinson ID, et al. **Magnetic resonance spectroscopic abnormalities in sporadic and variant Creutzfeldt-Jakob disease.** *Clin Radiol* 2003;58:148–53
22. Graham GD, Petroff OA, Blamire AM, et al. **Proton magnetic resonance spectroscopy in Creutzfeldt-Jakob disease.** *Neurology* 1993;43:2065–68
23. Behar KL, Boucher R, Fritch W, et al. **Changes in N-acetylaspartate and myo-inositol detected in the cerebral cortex of hamsters with Creutzfeldt-Jakob disease.** *Magn Reson Imaging* 1998;16:963–68
24. Konaka K, Kaido M, Okuda Y, et al. **Proton magnetic resonance spectroscopy of a patient with Gerstmann-Straussler-Scheinker disease.** *Neuroradiology* 2000;42:662–65
25. Lim CC, Tan K, Verma KK, et al. **Combined diffusion-weighted and spectroscopic MR imaging in Creutzfeldt-Jakob disease.** *Magn Reson Imaging* 2004;22:625–29
26. Cordery RJ, Macmanus D, Godbolt A, et al. **Short TE quantitative proton magnetic resonance spectroscopy in variant Creutzfeldt-Jakob disease.** *Eur Radiol* 2006;16:1–7. Epub 2006 Jan 12
27. Broom KA, Anthony DC, Lowe JP, et al. **MRI and MRS alterations in the preclinical phase of murine prion disease: association with neuropathological and behavioural changes.** *Neurobiol Dis* 2007;26:707–17. Epub 2007 Apr 5
28. Mittal S, Farmer P, Kalina P, et al. **Correlation of diffusion-weighted magnetic resonance imaging with neuropathology in Creutzfeldt-Jakob disease.** *Arch Neurol* 2002;59:128–34
29. Parchi P, Giese A, Capellari S, et al. **Classification of sporadic Creutzfeldt-Jakob disease based on molecular and phenotypic analysis of 300 subjects.** *Ann Neurol* 1999;46:224–33
30. Brandel JP, Heath CA, Head MW, et al. **Variant Creutzfeldt-Jakob disease in France and the United Kingdom: evidence for the same agent strain.** *Ann Neurol* 2009;65:249–56
31. Billette de Villemeur T, Gelot A, Deslys JP, et al. **Iatrogenic Creutzfeldt-Jakob disease in three growth hormone recipients: a neuropathological study.** *Neuropathol Appl Neurobiol* 1994;20:111–17
32. Tschampa HJ, Kallenberg K, Urbach H, et al. **MRI in the diagnosis of sporadic Creutzfeldt-Jakob disease: a study on inter-observer agreement.** *Brain* 2005; 128(pt 9):2026–33. Epub 2005 Jun 15
33. Young GS, Geschwind MD, Fischbein NJ, et al. **Diffusion-weighted and fluid-attenuated inversion recovery imaging in Creutzfeldt-Jakob disease: high sensitivity and specificity for diagnosis.** *AJNR Am J Neuroradiol* 2005; 26:1551–62
34. Shiga Y, Miyazawa K, Sato S, et al. **Diffusion-weighted MRI abnormalities as an early diagnostic marker for Creutzfeldt-Jakob disease.** *Neurology* 2004; 63:443–49
35. Meissner B, Kallenberg K, Sanchez-Juan P, et al. **Isolated cortical signal increase on MR imaging as a frequent lesion pattern in sporadic Creutzfeldt-Jakob disease.** *AJNR Am J Neuroradiol* 2008;29:1519–24
36. Fulbright RK, Hoffmann C, Lee H, et al. **MR imaging of familial Creutzfeldt-Jakob disease: a blinded and controlled study.** *AJNR Am J Neuroradiol* 2008; 29:1638–43